Human Molecular Genetics, 2015, Vol. 24, No. 8 2318–2329

doi: 10.1093/hmg/ddu749
Advance Access Publication Date: 9 January 2015
Original Article

ORIGINAL ARTICLE

Characterization of the mutational landscape of anaplastic thyroid cancer via whole-exome sequencing

John W. Kunstman[1,2,†], C. Christofer Juhlin[1,6,†], Gerald Goh[3,4,†], Taylor C. Brown[1,2], Adam Stenman[6], James M. Healy[1,2], Jill C. Rubinstein[1,2], Murim Choi[3,4], Nimrod Kiss[6], Carol Nelson-Williams[3,4], Shrikant Mane[3], David L. Rimm[5], Manju L. Prasad[5], Anders Höög[6], Jan Zedenius[7], Catharina Larsson[6], Reju Korah[1,2], Richard P. Lifton[3,4] and Tobias Carling[1,2,*]

[1]Yale Endocrine Neoplasia Laboratory, [2]Department of Surgery, [3]Department of Genetics, [4]Howard Hughes Medical Institute and [5]Department of Pathology, Yale School of Medicine, New Haven, CT 06520, USA, [6]Department of Oncology–Pathology and [7]Department of Molecular Medicine and Surgery, Karolinska Institutet, Karolinska University Hospital CCK, SE-171 76 Stockholm, Sweden

*To whom correspondence should be addressed at: Yale School of Medicine, 333 Cedar Street, FMB130A, Box 208062, New Haven, CT 06520, USA. Tel: +1 2037372036; Fax: +1 2037852498; Email: tobias.carling@yale.edu

Abstract

Anaplastic thyroid carcinoma (ATC) is a frequently lethal malignancy that is often unresponsive to available therapeutic strategies. The tumorigenesis of ATC and its relationship to the widely prevalent well-differentiated thyroid carcinomas are unclear. We have analyzed 22 cases of ATC as well as 4 established ATC cell lines using whole-exome sequencing. A total of 2674 somatic mutations (121/sample) were detected. Ontology analysis revealed that the majority of variants aggregated in the MAPK, ErbB and RAS signaling pathways. Mutations in genes related to malignancy not previously associated with thyroid tumorigenesis were observed, including *mTOR*, *NF1*, *NF2*, *MLH1*, *MLH3*, *MSH5, MSH6, ERBB2, EIF1AX* and *USH2A*; some of which were recurrent and were investigated in 24 additional ATC cases and 8 ATC cell lines. Somatic mutations in established thyroid cancer genes were detected in 14 of 22 (64%) tumors and included recurrent mutations in *BRAF*, *TP53* and *RAS*-family genes (6 cases each), as well as *PIK3CA* (2 cases) and single cases of *CDKN1B, CDKN2C*, *CTNNB1* and *RET* mutations. *BRAF* V600E and *RAS* mutations were mutually exclusive; all ATC cell lines exhibited a combination of mutations in either *BRAF* and *TP53* or *NRAS* and *TP53*. A hypermutator phenotype in two cases with >8 times higher mutational burden than the remaining mean was identified; both cases harbored unique somatic mutations in *MLH* mismatch-repair genes. This first comprehensive exome-wide analysis of the mutational landscape of ATC identifies novel genes potentially associated with ATC tumorigenesis, some of which may be targets for future therapeutic intervention.

Introduction

Anaplastic thyroid carcinoma (ATC) is a rare endocrine malignancy with therapeutic options of limited effectiveness. In contrast to the much more common malignancies of the thyroid follicular epithelium, such as papillary or follicular thyroid cancers (collectively known as 'well-differentiated thyroid

†The authors wish it to be known that, in their opinion, the first three authors should be regarded as joint First Authors.
Received: November 26, 2014. **Revised:** November 26, 2014. **Accepted:** December 29, 2014

cancers'—WDTC) which boast excellent cure rates and long-term survival, prognosis in ATC patients is exceedingly poor, nearly uniformly fatal, and has changed little in the past half century. In the USA, ATC is responsible for 1–2% of all thyroid cancers, but accounts for over 50% of deaths attributable to thyroid malignancy (1,2). Over 80% of patients present with loco-regional invasion and approximately half have distant metastases at the time of diagnosis (3–5). Considering the explosive clinical course of ATC, the recommended therapy is generally aggressive multimodal treatment for most patients (4). Despite maximal intervention, the median survival time is <6 months in most series, and cancer-specific mortality at 1 year exceeds 80% (4,6,7). The dismal prognosis and high prevalence of distant disease at the time of diagnosis highlights the urgent need for novel, targeted systemic treatments for ATC.

Approximately 20–25% of patients with ATC have a history of a previous WDTC and an additional 20–30% have a coexisting WDTC found following surgery for ATC (3,4,8,9). Although ATC can also arise *de novo* or in the setting of chronic goiter in occasional patients, these data suggest that a significant fraction of ATC cases are the result of progression from WDTC. Furthermore, genetic analysis of ATC has characterized frequent somatic mutations in several genes such as *BRAF* and *RAS* that are commonly mutated in WDTC as well, implying a common initial tumorigenic pathway (10–12). Mutations unique to ATC, in genes such as *TP53*, *CTNNB1* and others, are thought to be involved in dedifferentiation and progression to ATC. However, due to the rarity of ATC and correspondingly small sample size of most studies evaluating its genetic landscape, conclusively determining the incidence and impact of these mutations is difficult. For example, *CTNNB1* mutations have been variably observed at a rate of 0–61.3% of ATC cases (13–15). Similarly, widespread copy number and structural genomic instability have been repeatedly demonstrated in ATC with copy number gain present in over 80% of tumors, but wide spectrum of variation reported coupled with small sample sizes limit the generalizability of these studies (2,16). While current knowledge of the molecular pathogenesis of ATC has led to several clinical trials of existing targeted pharmaceuticals, the results have thus far not shown dramatic improvements in outcomes and the precise molecular mechanisms of ATC dedifferentiation and tumorigenesis remain unknown (17–19), although individual successes have been described (20,21).

Whole-exome capture coupled with next-generation sequencing technology is a proven method for identifying functionally relevant genetic variants underlying both Mendelian and complex disease states, such as neoplasia (22–24). The ability of whole-exome sequencing (WES) to resolve single-nucleotide variants is particularly suited for characterizing previously unknown drivers of tumorigenesis and survey the landscape of somatic mutations present in a malignancy (25,26). Furthermore, WES has been successfully utilized in the clinical environment for both genetic diagnosis and tumor genotyping (23,27,28); a possibly useful application in ATC, where conventional cancer therapies are largely ineffective and targeted therapies have not been widely applied but have been shown to be beneficial in individual cases. Thus, we hypothesized that WES would be an ideal platform to (i) better characterize the mutational landscape of ATC, (ii) identify novel potential driver mutations for further study in ATC tumorigenesis and (iii) detect possible candidates for targeted therapy in patients with ATC. Accordingly, we applied WES to a cohort of 22 unique cases of ATC and four established ATC cell lines in an effort to further these goals.

Results

Exome sequencing cohort

Demographic and pathologic information describing the exome sequencing cohort are shown in Table 1. Thirteen patients (59%) were women, nine (41%) were men and the mean age at surgery was 73 years (median 74 years). Tumor tissue from 19 of the patients (86%) were derived from primary tumor tissue, whereas three patients (14%) had previously undergone total thyroidectomy for papillary thyroid cancer and ATC specimens were obtained during subsequent procedures for recurrent disease or palliative purposes. Thirteen patients (59%) presented with distant metastases at diagnosis. Eight patients had been treated with neoadjuvant external beam irradiation. Ten patients had demonstrable evidence of concurrent or previous WDTC in either the ipsi- or contralateral thyroid lobe, nine with papillary thyroid cancer and one with follicular thyroid cancer.

Whole-exome sequencing

In the 22 matched tumor/normal pairs that underwent WES, a total of 2674 somatic variants were identified, 1972 of which were non-synonymous (74%). In total, 68% constituted coding missense mutations, 5% non-sense mutations and 1% were exon–intron boundary mutations. The number of somatic variants per tumor ranged from 4 to 1805, with a mean number of total and non-synonymous variants of 121.5 and 89.6 per tumor, respectively. Two samples demonstrated a significantly higher mutation burden compared with all other samples (T2—253 mutations, T11—1805 mutations). When samples T2 and T11 were excluded, the mean number of total and non-synonymous variants was 30.8 and 23.7 per tumor, respectively. An overview of the WES results by sample is shown in Figure 1, and a detailed list of the sequencing data for all 22 cohort tumor-normal pairs is included in Supplementary Material, Tables S1 and S2. The percentage of reads on target was 66% and 65% for tumor and normal tissue, respectively, and the percentage of bases covered >20 times was 96% (tumor) and 92% (normal tissue). Tumor samples were deliberately sequenced to a greater depth than normal tissue (mean 264 and 138 reads/sample, respectively) in order to minimize the impact of the perceived lower quality of DNA libraries derived from fresh-frozen, paraffin-embedded (FFPE) samples (T1–T15) and also to maximize detection of heterozygous mutations in tumor samples admixed with adjacent normal tissue. Thirty mutations identified by exome sequencing throughout the cohort were selected for confirmatory Sanger sequencing. The mutations selected for confirmation were chosen based on perceived relevance in tumorigenesis, availability of sample for confirmatory studies and to ensure mutations from multiple FFPE-derived samples were confirmed. As expected based on confirmatory sequencing from prior whole exome studies, 29 of 30 (96.7%) mutations examined were confirmed when subjected to Sanger sequencing (Supplementary Material, Table S3).

Potential novel driver gene mutations

While a majority of cases harbored somatic mutations in known thyroid malignancy-related genes (discussed below), 16 different cancer-related genes denoted as 'driver genes' by Vogelstein *et al.* (29) not typically identified as drivers of thyroid malignancy were found to be present among the studied tumors. Several of these mutations were present in multiple samples and are strongly correlated with non-thyroidal malignancies, such as *NF1, mTOR*

Table 1. Clinical characteristics of ATC tumor samples subjected to WES

Case	Source	Age	Presentation	Primary tumor size	Nodal stage	Metastases at diagnosis	Alive?	Survival (months)	Additional thyroid disease?
T1	FFPE	53	Neck mass, cord paralysis	5.0 cm	N0	None	Yes	50.9	No
T2	FFPE	70	Stridor, dyspnea	Debulking only	N1b	Bone	No	2.8	No
T3	FFPE	72	Surveillance ultrasound	N/A	N1b	Lung, chest wall	No	24.1	WDTC
T4	FFPE	70	Dysphagia	8.0 cm	N1b	Lung	N/A	N/A	Goiter
T5	FFPE	61	Neck mass	5.8 cm	N1b	Lung, brain, retroperitoneum	No	0.9	No
T6	FFPE	45	Neck mass	8.0 cm	N1b	None	No	11.3	No
T7	FFPE	89	Dysphagia	4.5 cm	Nx	Lung, chest wall	No	1	WDTC
T8	FFPE	78	Neck mass	6.0 cm	N1a	Lung	Yes	40.3	Graves' disease
T9	FFPE	59	Neck mass	7.5 cm	N1a	None	No	4.3	No
T10	FFPE	59	Dysphagia	N/A	N1b	Lung, chest wall	No	24.9	WDTC
T11	FFPE	65	Neck mass	8.0 cm	Nx	Lung	No	39.9	Goiter, WDTC
T12	FFPE	93	Airway collapse	8.0 cm	Nx	Lung	No	0.8	WDTC
T13	FFPE	75	Neck mass	3.7 cm	N1b	Lung	N/A	N/A	No
T14	FFPE	63	Hemoptysis	N/A	N1b	Lung, adrenal	N/A	N/A	WDTC
T15	FFPE	79	Stridor, dyspnea	Debulking only	Nx	Lung, liver	N/A	N/A	No
T16	Fresh Frozen	77	Neck mass	7.0 cm	Nx	Lung	No	3	WDTC
T17	Fresh Frozen	83	Neck mass	7.0 cm	Nx	None	No	11	Goiter
T18	Fresh Frozen	82	Neck mass	4.0 cm	Nx	N/A	No	1	WDTC
T19	Fresh Frozen	84	Neck mass	5.0 cm	N1b	None	No	3	No
T20	Fresh Frozen	72	Neck mass, dyspnea	10.0 cm	Nx	None	No	1	Goiter
T21	Fresh Frozen	89	Neck mass	8.0 cm	N1b	None	No	0.5	WDTC
T22	Fresh Frozen	85	Neck mass	4.0 cm	Nx	None	No	4	WDTC

FFPE, fresh-frozen paraffin-embedded; N/A, not available (lost to follow-up); WDTC, well-differentiated thyroid cancer.

(two cases each), *ERBB2*, *DAXX*, *MLL2*, and *NOTCH2* (one case each —Fig. 1). Cases T2 and T11, which exhibited a 'hypermutator phenotype' with a somatic mutation frequency well above the average were found to have missense and non-sense somatic mutations in evolutionary conserved positions of the mismatch repair (MMR) genes *MLH1* (T2) and *MLH3* (T11) (Table 2). Case T11, which also exhibited a mutation in mutS homolog gene *MSH5*, had 1805 somatic mutations compared with 253 in Case T2. These mutations were unique to cases T2 and T11 and the mutational burden of these two cases combined comprises 77% of the total somatic burden across the entire cohort.

Novel recurrently mutated COSMIC genes

COSMIC genes found to be recurrently mutated that have not previously been described in ATC development included four cases of non-synonymous *USH2A* missense mutations (4/22; 18%). Additionally, three cases with mutations in *EIF1AX* and *HECTD1* were found (3/22; 14%). These are summarized in Figure 1, Table 2 (*USH2A*, *EIF1AX*), and Supplementary Material, Table S2 (*HECTD1*).

ATC-related gene mutations

Multiple genes previously found to be involved in thyroid neoplasia demonstrated somatic mutations in the study group. These findings are summarized in Table 3 and include several well-described oncogenes and tumor suppressors. The most common recurrently mutated genes were *TP53* and *BRAF* with six cases each, followed by *NRAS* (3 cases), *KRAS* (2 cases), *PIK3CA* (2 cases) as well as *HRAS*, *CDKN1B*, *CDKN2C*, *CTNNB1*, *HRAS* and *RET* (one case each, Fig. 1, Table 3). Previously recognized ATC-related recurrent mutations present in the cohort included *BRAF* V600E (six cases), *NRAS* Q61R (two cases) and *PIC3CA* H1047R/L (one case each). The mean number of single-nucleotide variants in tumors harboring *BRAF* V600E mutations versus *RAS* mutations was 47.8 (±31.5) versus 22.2 (±6.7). For tumors harboring neither *BRAF* nor *RAS* mutations, the mean number of single-nucleotide variants (SNVs) was 24.5 (±18.3) (comparison of three groups; *P*-value 0.09). Previously reported frequencies of commonly described ATC gene variants are compared with the frequencies described here in Supplementary Material, Table S4.

Five cases did not exhibit somatic mutations in either the ATC-related or novel ATC gene variant gene groups (Fig. 1), and the mutational status of these cases are summarized in Supplementary Material, Table S5. The mean number of mutations present among these five cases was 12.4 (range 4–22). A subset of the cases (T6, T8) did exhibit damaging mutations with concurrent loss of heterozygosity (LOH) in COSMIC genes with largely unknown functions. The recent discoveries of *RASAL1* as a thyroid-specific tumor suppressor gene with a mutational frequency of 17% in ATC (30) and the role of ALK rearrangements in thyroid tumorigenesis (31,32) prompted investigation of whether *RASAL1* and *ALK* mutations were present in the cohort. No somatic mutations in *ALK* were found; however, a missense mutation in *RASAL1* (R774C) was identified in case T11 (Fig. 1).

Gene ontology and pathway analyses

Using the DAVID (Database for Annotation, Visualization and Integrated Discovery) Bioinformatics Resources 6.7 database for identification of enriched biological processes in the pool of somatically altered genes, wide and generic ontology terms were identified. These included metabolic processes, intracellular signaling, phosphorylation and apoptosis. Further analyses using

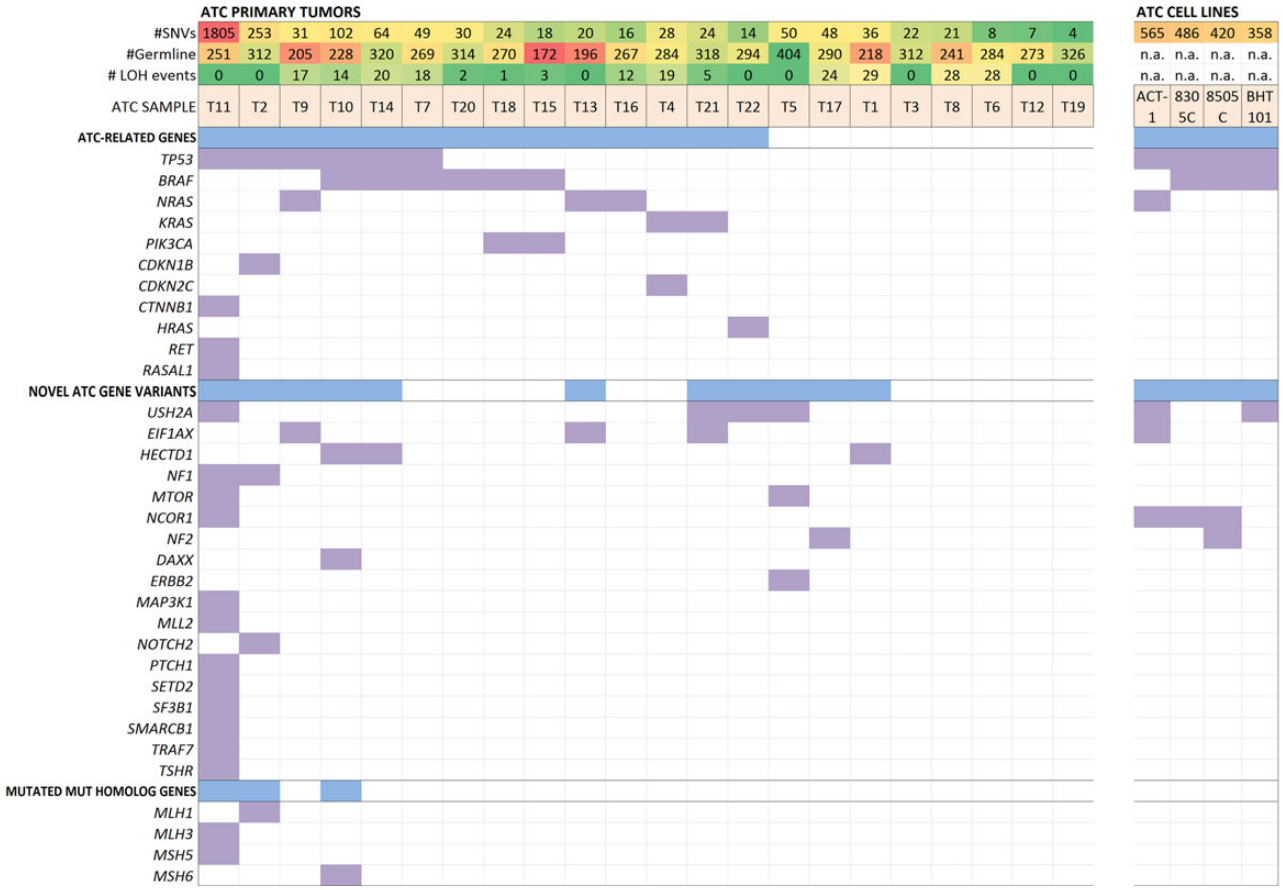

Figure 1. Overall mutational profile of the 22 ATCs studied by exome sequencing. All panels are aligned with vertical tracks representing 22 individuals with ATC (left) and 4 established ATC cell lines (right). The underlying heatmap shows the distribution of somatic coding mutations in thyroid malignancy-related genes, novel ATC gene variants [established driver genes as suggested by Vogelstein *et al.* (24) or recurrently mutated COSMIC genes found in ≥3 samples], and finally mutated Mut homolog genes in which a correlation to the amount of mutational rate was observed.

Table 2. Summary of individual mutations and associated protein coding change in non-synonymous mut homolog genes, *USH2A*, and *EIF1AX* among all ATC tissue samples assayed

Case	Gene	Location	Mutation (AA)	Position (AA/total AA)	*P*-value	Nucleotide position	Nucleotide change	PolyPhen2 score
T2	*MLH1*	Chr3	I19M	19/756	1.16E−31	37 010 099	C>G	1
T3	*MLH1*	Chr3	I68M	68/756	2.63E−21	37 013 201	C>G	1
T4	*MLH1*	Chr3	Q60X	60/756	8.23E−18	37 013 175	C>T	Truncating
T11	*MLH3*	Chr14	L264V	264/1429	5.10E−08	74 585 322	G>C	0.968
T12	*MSH5*	Chr6	A199V	199/822	4.43E−06	31 819 953	C>T	0.999
T10	*MSH6*	Chr2	D736H	736/1360	9.08E−06	47 880 832	G>C	1
T5	*USH2A*	Chr1	I2189V	2189/5202	2.18E−22	214 238 944	T>C	0
T11	*USH2A*	Chr1	D798V	798/5202	2.79E−05	214 486 966	T>A	0.921
T21	*USH2A*	Chr1	E4571K	4571/5202	6.33E−13	213 914 165	C>T	0.549
T22	*USH2A*	Chr1	L1727F	1727/5202	2.08E−34	214 323 540	G>A	0.961
T9	*EIF1AX*	ChrX	Ex-in boundary	1 bp upstream of exon 6	1.14E−88	20 058 647	C>G	Splice site
T13	*EIF1AX*	ChrX	G9R	9/144	1.40E−15	20 066 653	C>G	0.996
T21	*EIF1AX*	ChrX	P2R	2/144	2.57E−12	20 069 675	G>C	0.028

AA, amino acid.

KEGG (Kyoto Encyclopedia of Genes and Genomes) pathway annotations identified several pathways with significant representation in the ATC cohort, including general pathways in cancer, MAPK kinase and ErbB pathways as enriched among the mutated genes. The involvement of the MAPK kinase and ErbB pathways were further characterized and validated using an independent ontology analysis (Genomatix Pathway System), yielding *P*-values of 2.01e−6 and 6.88e−5, respectively. This analysis identified somatic mutations among the tumor cohort in both the MAPK/ERK pathway (*BRAF*, *HRAS*, *KRAS*, *NRAS*, *RAF1*, *AKT2* and *PIK3CA*)

Table 3. Overview of somatic mutations across all analyzed ATC tissue samples annotated in the COSMIC (Catalog of Somatic Mutations in Cancer) database ($n = 22$)

Gene	Location (cytoband)	No. of cases	Mutation(s) observed	Mutation type	No. with LOH	% tumors mutated in COSMIC[a]
All genes with recurrent mutations						
BRAF	7q34	6	V600E	Missense	None	19.61%
NRAS	1p13.2	3	Q61R/K	Missense	None	5.73%
PIK3CA	3q26.32	2	H1047R/L	Missense	None	11.85%
Recurrently mutated genes ($n \geq 3$)						
TP53	17p13.1	6	Various	Various	LOH (2/6)	29.00%
BRAF	7q34	6	V600E	Missense	None	19.61%
MUC16	19p13.2	4	Various	Various	None	9.46%
USH2A	1q41	4	Various	Various	None	9.15%
GPR112	Xq26.3	4	Various	Various	None	4.11%
NRAS	1p13.2	3	Q61R/K	Missense	None	5.73%
PCDH15	10q21.1	3	Various	Various	None	4.80%
LRP1	12q13.3	3	Various	Missense	None	3.80%
KIAA1109	4q27	3	Various	Missense	LOH (1/3)	3.76%
EIF1AX	Xp22.12	3	Various	Various	None	0.25%
HECTD1	14q12	3	Various	Missense	None	1.60%
Genes with damaging mutations + LOH						
NF2	22q12.2	1	E103X	Non-sense	LOH	7.57%
MPDZ	9p23	1	Q124X	Non-sense	LOH	1.82%
OR8K3	11q12.1	1	R292X	Non-sense	LOH	1.04%
SMARCAL1	2q35	1	Q34X	Non-sense	LOH	0.99%
C3orf77	3p21.31	1	W1446X	Non-sense	LOH	0.55%
EIF5A2	3q26.2	1	S44X	Non-sense	LOH	0.22%

LOH, loss of heterozygosity.
[a]Mutational frequency as reported in COSMIC in February 2014.

and the ErbB pathway (*MAPK10*, *ERBB2*, *ERBB3*, *RAF1*, *RAC1* and *NF2*) (Fig. 2). Additional analysis using DAPPLE (Disease Association Protein-Protein Link Evaluator) version 2.0 to examine the significance of protein–protein interactions among the gene products of those genes identified as mutated by exome sequencing was performed. Cases T2 and T11 were excluded from this analysis as well as the gene ontology analysis as they harbored a much greater mutational burden due to mutations in the mismatch repair process (described above). A pattern was observed in which proteins involved in the ErbB/RAS/MAPK signaling pathways separated from apoptosis-related pathways (Supplementary Material, Fig. S1).

Exome sequencing of ATC cell lines

The results from the exome sequencing of four established ATC cell lines are detailed in Figure 1 and Supplementary Material, Table S6. The number of mutations ranged from 358 (BHT101) to 565 (ACT1), averaging 457 mutations per cell line. All four cell lines exhibited mutations in *TP53*. Three cell lines were found to have the *BRAF* V600E mutation (8305C, 8505C, BHT101). The remaining cell line (ACT1) had mutations in *NRAS* and *EIF1AX*. Furthermore, ACT1 and BHT101 both exhibited *USH2A* mutations.

LOH and copy number variation analyses

A schematic overview of the LOH profile of the 22 ATCs studied is shown in Figure 3. In general, LOH events were most frequently identified in chromosomes 9p, 13p and 22q, averaging 40% of the cases. Eight of the ATCs had discernible copy number variations (CNVs), and there were no significant focal or arm-level CNVs from the GISTIC (Genomic Identification of Significant Targets in Cancer) analysis.

Correlations to clinical characteristics

The mean somatic mutation burden for the group that received neoadjuvant external radiotherapy ($n = 8$) was 51.6 mutations, compared with the 161.5 mutations seen in the group that did not receive neoadjuvant treatment ($n = 14$; $P = $ NS). However, when excluding the hypermutator tumors T2 and T11 (did, and did not, receive neoadjuvant radiotherapy, respectively), almost comparable levels were seen (35.1 versus 22.9 mutations respectively; $P = $ NS). Furthermore, no significant correlations were seen between number of somatic mutations and length of survival (Spearman's correlation $r = 0.169$, $P = 0.592$), lymph node status (Kruskal–Wallis $P = 0.909$, ANOVA $P = 0.800$) or metastases at presentation (t-test $P = 0.250$). There was no statistically significant difference in the number of mutations observed in the FFPE- versus fresh-frozen-derived tissues subjected to exome sequencing. All described correlations remained insignificant when cases with a hypermutator phenotype were excluded.

Validation cohort analysis

To further examine the novel mutations discussed above in *mTOR* and *ERBB2* that could have significant clinical impact, a validation cohort of 24 primary ATC cases and 8 ATC cell lines were subjected to targeted Sanger sequencing of the relevant mutation loci. In addition, *EIF1AX*, recently shown to be a potential driver in papillary thyroid carcinoma (33) and was one of the most frequent recurrently mutated novel genes among the exome sequencing cohort in the current study (three primary tumors and

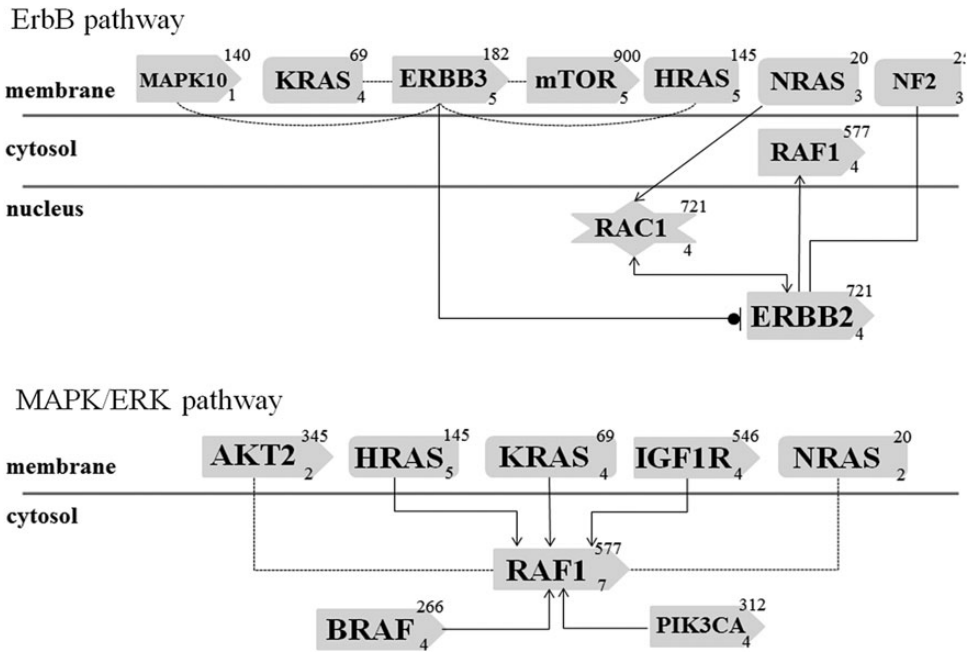

Figure 2. Simplistic overview of the top two mutation-enriched transduction signaling pathways in ATC as according to the Genomatix Pathway System. The ErbB (top) and MAPK/Erk (bottom) signaling pathways are illustrated with each mutated gene depicted. Gene products are drawn as rounded rectangles, snip-sided rectangles denote proteins with kinase properties and star-shaped symbols denote co-factors. The top right number denotes the number of sources for a chemical association with established molecules (for therapeutic purposes), the lower right number refers to the number of established interactions within the pathway in addition to the drawn association. Filled lines with arrows denote an activating effect; filled lines with stop line and circle denote inhibitory effect. Dotted lines indicate evidence at the level of co-citation, in contrast to filled lines which indicate evidence at expert-curation level.

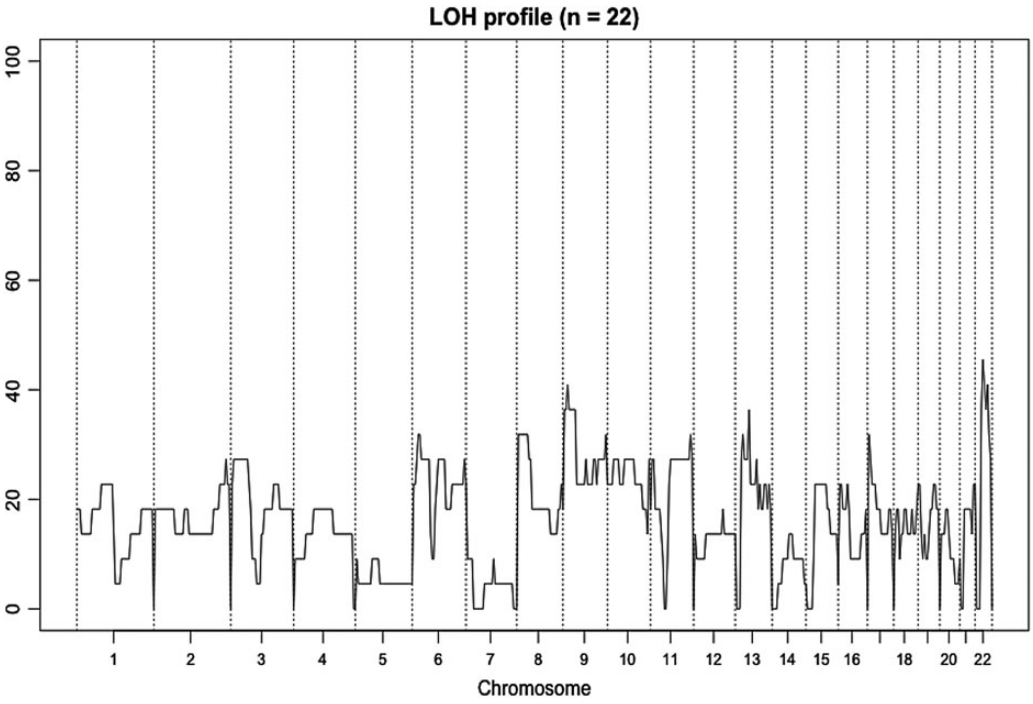

Figure 3. LOH profile for the exome cohort. The graph depicts the overall LOH profile of the 22 ATC cases. Chromosome numbers are annotated on the *x*-axis and frequency of LOH on the *y*-axis. LOH events were most frequently identified in chromosomes 9p, 13p and 22q, averaging 40% of the cases.

one cell line), was also selected for further examination, as was the well-recognized *BRAF* V600E mutation.

A mutation in *EIF1AX* (Chr X:20058647; G>A) was found in ATC cell line c643, which corresponds to the identical chromosomal position of a heterozygous somatic mutation found in exome sample T9 (Chr X:20058647; G>C, Supplementary Material, Tables S2 and S7). This mutation, a single base pair upstream from the splice site of exon 6, is predicted as damaging by computational analysis (34). Furthermore, a recurrent SNP in the 5′ UTR of *EIF1AX* (rs201653081, C>T) four base pairs upstream of exon 1

(Chr X:20141644) were observed in two validation cohort samples; greater than the expected minor allele frequency of 0.24%. No additional mutations at the examined *mTOR* or *ERBB2* loci were found in the validation cohort (R164Q/M2327I and D387N, respectively). Five *BRAF* V600E mutations were found; four were within the ATC cell lines and served as positive controls for the Sanger sequencing as they have been previously described (35).

Discussion

The dismal prognosis of ATC is directly related to the ineffectiveness of mainstream treatment options and the incomplete understanding of the mechanisms of ATC tumorigenesis. This study sought to address these challenges using an exome-wide sequencing approach in 22 cases of ATC to survey the frequency of established genetic events in tumorigenesis, identify potential novel driver genetic events and characterize future candidates for targeted therapy. In summary, the results confirm that the genetic background of ATC is highly heterogeneous, but several novel genetic events not previously described in ATC were demonstrated. Some of these, such as mutations *mTOR*, *NF1*, or *ERBB2*, are particularly intriguing as these genes have been targeted previously by pharmaceuticals currently in clinical or experimental use. Additionally, two tumors were found to have defects in a mismatch repair genes and feature a hypermutator phenotype, a previously poorly characterized finding in ATC. Finally, the mutational landscape of the cohort was described with known thyroid malignancy genes present at varying frequencies in most, but not all, ATC cases.

The prototypic progression to ATC can be considered as a multi-step de-differentiation process in many cases, arising from a pre-existing WDTC such as papillary thyroid cancer or follicular thyroid cancer. This is best illustrated by the frequent observation of mutations in the *BRAF* and *RAS* oncogenes in ATC. The well-described *BRAF* V600E variant is the most common mutation in papillary thyroid cancer, while *NRAS/KRAS/HRAS* variants are commonly found in follicular thyroid cancer. In the current study, the observed frequencies for the *BRAF* V600E and *RAS* mutations (27% for both) mirrored the prevalence reported in previous manuscripts [Supplementary Material, Table S4 (12,15,36–38)]. As *BRAF* and *RAS* mutations are thought to be the drivers for development of WDTC prior to ATC development, the prevalence of these two mutations in a particular ATC cohort would be expected to be static. The cumulative prevalence of ~50–60% for these two mutations in this and other ATC cohorts may represent the fraction of ATCs that genuinely arise from prior WDTCs. All *BRAF* mutations in the current study were found to be the V600E variant and were mutually exclusive with *RAS* mutations, presumably reflecting the underlying WDTC variant (papillary or follicular thyroid cancer, respectively). For instance, in six cases of ATC found to harbor the *BRAF* V600E mutation described here, four had either been treated for pre-existing PTC or were found to have concurrent PTC elsewhere in the thyroid following resection.

The mechanism by which de-differentiation results in progression from WDTC to ATC have been a topic of frequent study with accumulation of mutations in recognized malignancy-associated genes such as *TP53* and the phosphatidylinositol 3-kinase/Akt (PI3-K/Akt) and Ras/Raf/mitogen-activated protein kinase (Ras/Raf/MAPK) pathways being regularly mentioned (12,15,39). Indeed, half of the cases of ATC with *BRAF* V600E mutations in this cohort harbored coexisting mutations in *TP53*; mice with loss of *TP53* function with *BRAF* V600E mutations are known to develop ATC (40). Among those *BRAF* V600E cases that did not have *TP53* mutations, two-thirds demonstrated activating mutations in *PIK3CA* (H1047R/L in T15/T11). In a mouse model, *PIK3CA* H1047L is unable to drive thyroid tumorigenesis independently; however, in mice with both *PIK3CA* H1047L and *BRAF* V600E mutations, ATC will occur (41). Notably, in these ATC cases featuring *BRAF* V600E in coexistence with *PIK3CA* or *TP53* mutations, few, if any, mutations in other known ATC-related or COSMIC genes are observed.

Among cases harboring *NRAS/HRAS/KRAS* mutations, the de-differentiation process is less clear. Only a single *TP53* mutation (T9) and no *PIK3CA* mutations were observed. *RAS* mutations in thyroid cancer appear to be independently activating of the PI3K-Akt pathway (38), yet many such cases of WDTC do not progress to ATC. An intriguing candidate not previously reported in thyroid malignancy identified by exome sequencing is *EIF1AX*. This gene encodes an essential eukaryotic translation initiation factor and was observed to be recurrently mutated in half of ATC cases harboring *RAS* mutations. It was not observed in any cases without a coexisting *RAS* mutation, nor was it observed in any cases with *BRAF* V600E mutations. Two of the three mutations were missense and the third was at a splice site; all were predicted to be damaging (Table 2). Furthermore, cell line ACT-1, which features wild-type *BRAF* but mutant *NRAS*, also demonstrated the EIF1AX mutation in the same residue mutated in sample T21. Moreover, in the validation cohort assessed here, cell line c643 (known to be *BRAF* wild-type) demonstrated the same splice site mutation as sample T9 from the whole exome cohort mutations in *EIF1AX* have recently been identified (via WES) in a significant fraction of uveal melanomas (42). These mutations are postulated to be late events in melanoma progression and have prognostic significance (43,44). Moreover, the recently released analysis of the genetic landscape of papillary thyroid cancer by the Cancer Genome Atlas Research Network has also identified *EIF1AX* as a possible novel driver of thyroid tumorigenesis (33). While the contribution of *EIF1AX* to tumor progression remains unclear, it has been shown that increased *EIF1AX* activity triggers cell proliferation *in vitro* (45). As a recurrent event coexisting with *RAS*-mutated ATC cases, *EIF1AX* is an attractive target for further investigation.

ATC also appears to arise *de novo*, without previous overt signs of differentiated cancer (39). Potential driver mutations in ErbB pathway genes (*ERBB2* (D387N), *NF2* (E103X) and *mTOR* (R164Q) were identified in two cases. These three genes have driver properties based on experimental findings in unrelated tumor types, and both *ERBB2* (HER-2) and *mTOR* are overexpressed or mutated in various malignancies (46,47). The specific *ERBB2* and *mTOR* mutations described in T5 have not previously been annotated as COSMIC variants. The *ERBB2* D387N mutation is located in the extracellular domain; this region has unknown biological significance but is a commonly mutated domain in urothelial cancer (48). The truncating *NF2* mutation in Case T17 was found to overlap a region of LOH, implying that the bi-allelic inactivation of *NF2* in this case could represent a crucial event in progression of this tumor. Such alterations in the ErbB pathway alterations may potentially have an independent driver role in the development of ATC. Several additional recurrently mutated genes annotated in the COSMIC database previously not described in ATC were also identified. In addition to *EIF1AX* (discussed above), the most frequent were *USH2A* (four cases) and *HECTD1* (three cases). Of these cases, *USH2A* is of particular interest. The gene encodes uscherin, which is ubiquitously expressed and involved in extracellular matrix binding via basement membrane-based interaction with collagen IV and fibronectin. *USH2A* is a COSMIC-annotated gene with various frequencies of somatic

mutations observed in malignant lesions, and the gene was recently postulated to be one of the top 10 mutated genes across various human tumor types (49). Germline mutations in *USH2A* are associated with Usher syndrome type 2A (OMIM: 276901), a disorder characterized by hearing deficiencies and retinitis pigmentosa (50). Potential alterations in ECM or cellular adhesion functions merit close attention in highly invasive and metastatic tumors such as ATC.

Two ATC cases exhibited a 'hypermutator' phenotype that has been observed in other cancers but has not been described in ATC (51,52). The probable etiology of this phenotype is the presence of highly damaging MutL homolog mutations in both cases (*MLH1* in T2 and *MLH3* in T11; T11 also having an *MSH5* mutation). Damaging mutations in this family of genes results in hypermutability in both human cancers and experimental yeast models (53,54). A single case of ATC has been reported in an individual with hereditary nonpolyposis colon cancer (HNPCC—Lynch syndrome) (55). Both cases here demonstrated *TP53* mutations as well, but as both were *BRAF* and *RAS* wild-type, the MutL homolog mutations may be crucial contributors to tumor initiation or progression. A third case demonstrated a mutation in the *MutS* homolog *MSH6* (T10); this tumor did exhibit BRAF V600E.

Five ATC cases (23%) did not demonstrate somatic mutations in either known thyroid cancer-related genes or genes with known driver properties. The mechanism of ATC tumorigenesis in these samples is limited to speculation, but might be attributable to somatic mutations in COSMIC genes of unknown function (Supplementary Material, Table S5), alternatively due to epigenetic or genetic alterations such as gene fusions; this is noteworthy as several rearrangements are recognized to drive WDTC tumorigenesis, such as *RET*, *ALK* or *NTRK3* fusions in PTC and *PAX8/PPARγ* in FTC (33,39). Interestingly, the lack of potential driver mutations in 22.7% (5/22) cases in the exome sequencing cohort roughly mirrors the 15.3% (74/484) of cases found to harbor chromosomal rearrangements and translocations in a recent analysis of the genetic landscape of PTC (33). Regarding the most common previously reported gene variants characterized in ATC, significant heterogeneity exists in the reported frequency of mutation. However, no significant difference in the rate of *TP53*, *BRAF* or *RAS*-family mutations were observed when historical reports were compared with the frequencies observed in the current study (12,15,36–38,56) (Supplementary Material, Table S4). Garcia-Rostan *et al.* (57) initially reported mutations in exon 3 of *CTNNB1* occurred in 65.5% of ATCs; a statistically significant difference in prevalence compared with the single *CTNNB1* mutation is observed here (also in exon 3). However, subsequent reports have found that the rate of *CTNNB1* mutation seems to approximate the prevalence observed here (0–4.5% of ATC) (14,15). Other uncommon genetic events reported in thyroid malignancy were observed only rarely or not at all (such as mutations in *RASAL1, PTEN,* or *Akt*), likely due to the small sample size mandated by the rarity of ATC and the infrequency of these events (16,30,58).

Ontology analysis of all somatic mutations demonstrated during WES revealed clusters in the MAPK and RAS/ErbB pathways (Fig. 2). Prior studies had surmised the importance of these pathways in ATC tumorigenesis. However, a significant number of somatic mutations in genes associated with these pathways but previously not shown to be altered in ATCs were confirmed here. An overall enrichment of mutations in apoptosis-related genes was also appreciated. This persisted even when limiting analysis to COSMIC-annotated gene variants; presumably, these variants are involved in dedifferentiation as large-cohort landscape analyses of WDTC have not demonstrated similar findings. DAPPLE analysis confirmed the above findings; also identifying clusters in ErbB/RAS/MAPK pathway and apoptosis-related proteins (Supplementary Material, Fig. S1). This may correlate with the global up-regulation of TGF-β genes described by Pita *et al.* in ATC (15); as RAS/MAPK signaling is known to integrate with the TGF-β pathway to regulate transcriptional activity. This synergy appears to have a significant effect on gene expression in ATC and should be a topic for ongoing study (59,60).

Examination of the mutational landscape of the study cohort revealed several trends. Three broad, mutually exclusive groups of ATC can be characterized based on their defining mutation: (1) tumors harboring *BRAF* V600E, (2) tumors with mutations within Ras-family genes, (3) tumors without either *BRAF* or *Ras* mutations (non-*BRAF*/non-*Ras*). Presumably, the majority of tumors in Groups (1) and (2) arose from pre-existing WDTC; a subset of tumors in Group (3) may also have arisen from WDTC via driver mechanisms not completely detectable by exome sequencing (i.e. gene rearrangements) or by novel mechanisms suggested here (such as microsatellite instability). Within Groups (1) and (2), dedifferentiation occurs via a small number well-recognized mechanisms including additional mutations in genes such as *TP53*, *PIK3CA* and others; *EIF1AX* may be a novel driver within this group identified here by exome sequencing in ATC. Within the non-*BRAF*/non-*Ras* group of tumors, potential drivers of dedifferentiation including *NF1, ERBB2* and *MTOR* and hypermutator MLH mutations.

Although the genetic and epigenetic events that result in thyroid malignancy continue to be defined with increasing clarity, some patients with certain subtypes of thyroid cancer, such as ATC, persistently have dismal outcomes. Of the recognized or novel driver genes identified here, many have pharmaceuticals targeting their action already in clinical or research usage. While several intriguing findings meriting further investigation are described here, perhaps the most noteworthy conclusion from this study is the potential role for next-generation sequencing of all ATC cases upon diagnosis. Such an effort may identify candidates for empiric targeted therapy in order to mitigate the highly lethal burden of this disease.

Materials and Methods

Sample acquisition

The exome sequencing cohort included matched tumor and normal samples from 22 ATC cases. Regardless of tissue source, ATC samples are histologically heterogeneous as different areas of the tumor contain a mix of viable and necrotic tumor cells, normal parenchyma and stromal tissue. In order to maximize sample accrual, we utilized formalin-fixed, paraffin-embedded (FFPE) archival tumor samples for tissue acquisition for 15 out of 22 cases (T1–15; 68%). Recently, FFPE-derived tissue has been demonstrated to be viable for effective WES (61,62). These patients underwent surgical resection at Yale-New Haven Hospital (New Haven, CT, USA). Briefly, all surgical pathology reports containing 'anaplastic' and 'thyroid' search terms from 1988 to 2012 were manually reviewed and tissue blocks were obtained for appropriate cases. Blocks with adequate remaining tissue were sectioned and re-reviewed by an experienced pathologist to confirm the presence of ATC and matched normal tissue for WES. The histopathological diagnosis was established according to WHO classification. Three 1 mm tissue cores were obtained and post-core sectioning was performed and reviewed to ensure tissue fidelity. Paraffin was then enzymatically removed and genomic DNA was

extracted and sheared via sonication. Seven additional cases of ATC (T16–22, 32%) were obtained from fresh-frozen tissue samples with matched normal tissue from fresh-frozen thyroid ($n = 5$) or leukocyte DNA ($n = 2$) from the Karolinska University Hospital (Stockholm, Sweden). Genomic DNA was extracted using the DNeasy Blood and Tissue DNA isolation kit (Qiagen, Hilden, Germany) in accordance with the manufacturer's instruction. All fresh-frozen specimens were sectioned in parallel to the DNA extraction and subsequently re-analyzed by light microscopy to verify appropriate representation of tumor or normal tissue. The procurement of tissue and subsequent genomic analyses were approved by the Yale University Institutional Review Board, New Haven, CT, USA, and the local ethical review board at Karolinska Institutet, Stockholm, Sweden.

The validation cohort consisted of samples of fresh-frozen tissues from a total of 16 histologically confirmed ATCs collected at the Karolinska University Hospital, Stockholm, Sweden. Tissue samples were snap-frozen following resection and genomic DNA was extracted using the DNeasy Blood and Tissue DNA isolation kit (Qiagen, Hilden, Germany) in accordance with the manufacturer's instruction. Fourteen of sixteen tissue samples were examined and confirmed by an experienced endocrine pathologist to demonstrate adequate representation of ATC tumor cells (Supplementary Material, Table S7).

ATC cell lines

Four established ATC cell lines (8305C, 8505C, ACT-1 and BHT101) were also exome-sequenced in addition to the 22 matched pairs of ATC and normal tissues described above using identical methodology for DNA isolation. 8305C and 8505C were purchased from Sigma, MO, USA. BHT101 was purchased from DSMZ Germany, while ACT-1 was generously provided by R.E. Schweppe, University of Colorado School of Medicine, Aurora, CO, USA (originator—Naoyoshi Onoda, Osaka City University, Japan). Cell lines used for the exome analysis (8505C, 8305C, BHT101 and ACT-1) were authenticated to be distinct and of human ATC origin by short tandem repeat and single-nucleotide polymorphism array analysis (63). Additional ATC cell lines used for the validation cohort (Supplementary Material, Table S7) were kindly provided by Dr Nils-Erik Heldin (Uppsala University, Sweden). These lines were reported previously to be of human origin and authenticated by genotyping of short tandem repeats (35,64).

Exome capture, massively parallel sequencing and analysis

Genomic DNA samples generating an adequate high-quality library were subjected to exome capture and sequencing as previously described (23). Briefly, adaptors of known sequence were ligated to genomic DNA fragments which were amplified by ligation-mediated PCR and were then subjected to capture utilizing the NimbleGen 2.1M human exome array. Exome-specific DNA was eluted and then underwent 74 base paired-end sequencing on the Illumina HiSeq 2000 instrument according to the manufacturer's instructions. SAMtools was utilized for base calling and removal of PCR duplicates. Reads were then mapped to the human reference genome GRCh37/hg18 using the ELAND program. Significance of somatic variant calls was assessed by comparing reference and non-reference reads utilizing Fisher's exact test and were manually curated on a sample-by-sample basis to determine high-quality reads. Known variants in annotated databases were excluded and novel variants were evaluated for impact on transcriptional and/or translational processing as well as sequence conservation.

CNV prediction and LOH analysis

LOH loci were identified by comparing B allele frequencies (BAF) of a known array of SNPs in matched tumor and normal samples. Regions with apparent BAF shift were then manually curated to determine LOH. Comparative analysis of coverage depth between tumor and normal samples in 500 kb capture intervals was utilized to identify regions of somatic CNV. Significance was assessed by randomly distributing CNVs in >108 permutations and assessing the likelihood of observing the distribution by chance alone. Again, a false-discovery cut-off of <0.25 was considered significant. A GISTIC-like peel algorithm was utilized to assess the significance of individual CNV peaks.

Sequence validation

Thirty somatic mutations of interest were selected for validation via Sanger sequencing. Flanking primers were designed using an NCBI PrimerBlast (http://blast.ncbi.nlm.nih.gov) and genomic DNA was amplified via PCR and verified to be of correct size by agarose gel electrophoresis (Supplementary Material, Table S3). Putative mutations were sequenced using forward and reverse primers and confirmed by two independent reads. All cases in the validation cohort were analyzed for the demonstrated *mTOR* R164Q/M2327I, *ErbB2* D387N, *BRAF* V600E mutations defined during exome sequencing and the seven coding exons of *EIF1AX* were sequenced in a similar fashion. Chromatograms were analyzed using CodonCode Aligner software (CodonCode Corporation; Centerville, MA, USA).

Ontology analysis

We applied the DAVID Bioinformatics Resources 6.7 database (http://david.abcc.ncifcrf.gov) to aid in the identification of significantly altered biological processes and pathways among the 22 ATC cases. By using a functional annotation tool and a user-customized gene background, gene-annotation enrichment analyses as well as KEGG pathway mapping were performed. Significantly enriched GO terms and pathways were selected based on Benjamini-corrected *P*-values, to allow a balance between discovery of statistically significant genes and restriction of false-positive occurrences. Pathway analyses were also carried out using the Genomatix Pathway System (www.genomatix.de), in which information is extracted from public databases to present >400 canonical pathways as well as extended networks based on literature data rather than GO terms. We furthermore employed the Disease Association Protein-Protein Link Evaluator (DAPPLE—www.broadinstitute.org/mpg/dapple/dapple.php) to evaluate important physical associations between proteins encoded by mutated genes in the ATC cohort. The analysis was made allowing 10 000 permutations and a common interactor binding degree cut-off of 2. Associations are reported with the Bonferroni-corrected *P*-values representing the statistical significance of a number of network connectivity parameters reported in the literature.

Statistical analyses

Statistical calculations were carried out using the IBM SPSS Statistics 19 software (IBM, Armonk, NY, USA). Tests for normality of continuous variables were performed using the Shapiro–Wilk test, and Spearman's correlation, *t*-test, Kruskal–Wallis and

ANOVA tests were used to test for significance between various clinical parameters and overall mutational burden. *P*-values of <0.05 were considered as statistically significant.

Supplementary Material

Supplementary Material is available at *HMG* online.

Acknowledgements

The authors would like to thank Aruna Madan, MD, Lisa Ånfalk and John Overton, PhD for their invaluable assistance in sample collection, submission and assistance. Dr Robert Udelsman, MD, MBA, FACS, FACE, is thanked for his unwavering support of this project.

Conflict of Interest statement. The funding sources had no role in the design, conduct, or reporting of this study and the authors have no conflict of interest to report.

Funding

This work was supported by the Damon Runyon Cancer Research Foundation (T.C.); the Stockholm County Council (C.C.J.); the Swedish Cancer Society (C.C.J., J.Z.); the Swedish Research Council (C.L., A.S.); the Agency for Science, Technology and Research, Singapore (G.G.); and the Howard Hughes Medical Institute (R.P.L.).

References

1. Ragazzi, M., Ciarrocchi, A., Sancisi, V., Gandolfi, G., Bisagni, A. and Piana, S. (2014) Update on anaplastic thyroid carcinoma: morphological, molecular, and genetic features of the most aggressive thyroid cancer. *Int. J. Endocrinol.*, **2014**, 790834.
2. Smallridge, R.C., Marlow, L.A. and Copland, J.A. (2009) Anaplastic thyroid cancer: molecular pathogenesis and emerging therapies. *Endocr. Relat. Cancer*, **16**, 17–44.
3. McIver, B., Hay, I.D., Giuffrida, D.F., Dvorak, C.E., Grant, C.S., Thompson, G.B., van Heerden, J.A. and Goellner, J.R. (2001) Anaplastic thyroid carcinoma: a 50-year experience at a single institution. *Surgery*, **130**, 1028–1034.
4. Smallridge, R.C., Ain, K.B., Asa, S.L., Bible, K.C., Brierley, J.D., Burman, K.D., Kebebew, E., Lee, N.Y., Nikiforov, Y.E., Rosenthal, M.S. *et al.* (2012) American Thyroid Association guidelines for management of patients with anaplastic thyroid cancer. *Thyroid*, **22**, 1104–1139.
5. Sugitani, I., Miyauchi, A., Sugino, K., Okamoto, T., Yoshida, A. and Suzuki, S. (2012) Prognostic factors and treatment outcomes for anaplastic thyroid carcinoma: ATC Research Consortium of Japan cohort study of 677 patients. *World J. Surg.*, **36**, 1247–1254.
6. Kebebew, E., Greenspan, F.S., Clark, O.H., Woeber, K.A. and McMillan, A. (2005) Anaplastic thyroid carcinoma. Treatment outcome and prognostic factors. *Cancer*, **103**, 1330–1335.
7. Neff, R.L., Farrar, W.B., Kloos, R.T. and Burman, K.D. (2008) Anaplastic thyroid cancer. *Endocrinol. Metab. Clin. North Am.*, **37**, 525–538. xi.
8. Lam, K.Y., Lo, C.Y., Chan, K.W. and Wan, K.Y. (2000) Insular and anaplastic carcinoma of the thyroid: a 45-year comparative study at a single institution and a review of the significance of p53 and p21. *Ann. Surg.*, **231**, 329–338.
9. Venkatesh, Y.S., Ordonez, N.G., Schultz, P.N., Hickey, R.C., Goepfert, H. and Samaan, N.A. (1990) Anaplastic carcinoma of the thyroid. A clinicopathologic study of 121 cases. *Cancer*, **66**, 321–330.
10. Guerra, A., Di Crescenzo, V., Garzi, A., Cinelli, M., Carlomagno, C., Tonacchera, M., Zeppa, P. and Vitale, M. (2013) Genetic mutations in the treatment of anaplastic thyroid cancer: a systematic review. *BMC Surg.*, **13**(Suppl 2), S44.
11. Nikiforov, Y.E. (2004) Genetic alterations involved in the transition from well-differentiated to poorly differentiated and anaplastic thyroid carcinomas. *Endocr. Pathol.*, **15**, 319–327.
12. Santarpia, L., El-Naggar, A.K., Cote, G.J., Myers, J.N. and Sherman, S.I. (2008) Phosphatidylinositol 3-kinase/akt and ras/raf-mitogen-activated protein kinase pathway mutations in anaplastic thyroid cancer. *J. Clin. Endocrinol. Metab.*, **93**, 278–284.
13. Garcia-Rostan, G., Tallini, G., Herrero, A., D'Aquila, T.G., Carcangiu, M.L. and Rimm, D.L. (1999) Frequent mutation and nuclear localization of beta-catenin in anaplastic thyroid carcinoma. *Cancer Res.*, **59**, 1811–1815.
14. Kurihara, T., Ikeda, S., Ishizaki, Y., Fujimori, M., Tokumoto, N., Hirata, Y., Ozaki, S., Okajima, M., Sugino, K. and Asahara, T. (2004) Immunohistochemical and sequencing analyses of the Wnt signaling components in Japanese anaplastic thyroid cancers. *Thyroid*, **14**, 1020–1029.
15. Pita, J.M., Figueiredo, I.F., Moura, M.M., Leite, V. and Cavaco, B. M. (2014) Cell cycle deregulation and TP53 and RAS mutations are major events in poorly differentiated and undifferentiated thyroid carcinomas. *J. Clin. Endocrinol. Metab.*, **99**, E497–E507.
16. Liu, Z., Hou, P., Ji, M., Guan, H., Studeman, K., Jensen, K., Vasko, V., El-Naggar, A.K. and Xing, M. (2008) Highly prevalent genetic alterations in receptor tyrosine kinases and phosphatidylinositol 3-kinase/akt and mitogen-activated protein kinase pathways in anaplastic and follicular thyroid cancers. *J. Clin. Endocrinol. Metab.*, **93**, 3106–3116.
17. Sosa, J.A., Balkissoon, J., Lu, S.P., Langecker, P., Elisei, R., Jarzab, B., Bal, C.S., Marur, S., Gramza, A. and Ondrey, F. (2012) Thyroidectomy followed by fosbretabulin (CA4P) combination regimen appears to suggest improvement in patient survival in anaplastic thyroid cancer. *Surgery*, **152**, 1078–1087.
18. Nixon, I.J., Shaha, A.R. and Tuttle, M.R. (2013) Targeted therapy in thyroid cancer. *Curr. Opin. Otolaryngol. Head Neck Surg.*, **21**, 130–134.
19. Jin, N., Jiang, T., Rosen, D.M., Nelkin, B.D. and Ball, D.W. (2009) Dual inhibition of mitogen-activated protein kinase kinase and mammalian target of rapamycin in differentiated and anaplastic thyroid cancer. *J. Clin. Endocrinol. Metab.*, **94**, 4107–4112.
20. Wagle, N., Grabiner, B.C., Van Allen, E.M., Amin-Mansour, A., Taylor-Weiner, A., Rosenberg, M., Gray, N., Barletta, J.A., Guo, Y., Swanson, S.J. *et al.* (2014) Response and acquired resistance to everolimus in anaplastic thyroid cancer. *N. Engl. J. Med.*, **371**, 1426–1433.
21. Rosove, M.H., Peddi, P.F. and Glaspy, J.A. (2013) BRAF V600E inhibition in anaplastic thyroid cancer. *N. Engl. J. Med.*, **368**, 684–685.
22. Bilguvar, K., Ozturk, A.K., Louvi, A., Kwan, K.Y., Choi, M., Tatli, B., Yalnizoglu, D., Tuysuz, B., Caglayan, A.O., Gokben, S. *et al.* (2010) Whole-exome sequencing identifies recessive WDR62 mutations in severe brain malformations. *Nature*, **467**, 207–210.
23. Choi, M., Scholl, U.I., Ji, W., Liu, T., Tikhonova, I.R., Zumbo, P., Nayir, A., Bakkaloglu, A., Ozen, S., Sanjad, S. *et al.* (2009) Genetic diagnosis by whole exome capture and massively parallel DNA sequencing. *Proc. Natl Acad. Sci. USA*, **106**, 19096–19101.

24. Cromer, M.K., Starker, L.F., Choi, M., Udelsman, R., Nelson-Williams, C., Lifton, R.P. and Carling, T. (2012) Identification of somatic mutations in parathyroid tumors using whole-exome sequencing. *J. Clin. Endocrinol. Metab.*, **97**, E1774–E1781.
25. Zhao, S., Choi, M., Overton, J.D., Bellone, S., Roque, D.M., Cocco, E., Guzzo, F., English, D.P., Varughese, J., Gasparrini, S. *et al.* (2013) Landscape of somatic single-nucleotide and copy-number mutations in uterine serous carcinoma. *Proc. Natl Acad. Sci. USA*, **110**, 2916–2921.
26. Krauthammer, M., Kong, Y., Ha, B.H., Evans, P., Bacchiocchi, A., McCusker, J.P., Cheng, E., Davis, M.J., Goh, G., Choi, M. *et al.* (2012) Exome sequencing identifies recurrent somatic RAC1 mutations in melanoma. *Nat. Genet.*, **44**, 1006–1014.
27. Haimovich, A.D. (2011) Methods, challenges, and promise of next-generation sequencing in cancer biology. *Yale J. Biol. Med.*, **84**, 439–446.
28. Vater, I., Montesinos-Rongen, M., Schlesner, M., Haake, A., Purschke, F., Sprute, R., Mettenmeyer, N., Nazzal, I., Nagel, I., Gutwein, J. *et al.* (2014) The mutational pattern of primary lymphoma of the central nervous system determined by whole-exome sequencing. *Leukemia*, doi: 10.1038/leu.2014.264.
29. Vogelstein, B., Papadopoulos, N., Velculescu, V.E., Zhou, S., Diaz, L.A. Jr. and Kinzler, K.W. (2013) Cancer genome landscapes. *Science*, **339**, 1546–1558.
30. Liu, D., Yang, C., Bojdani, E., Murugan, A.K. and Xing, M. (2013) Identification of RASAL1 as a major tumor suppressor gene in thyroid cancer. *J. Natl Cancer Inst.*, **105**, 1617–1627.
31. Kelly, L.M., Barila, G., Liu, P., Evdokimova, V.N., Trivedi, S., Panebianco, F., Gandhi, M., Carty, S.E., Hodak, S.P., Luo, J. *et al.* (2014) Identification of the transforming STRN-ALK fusion as a potential therapeutic target in the aggressive forms of thyroid cancer. *Proc. Natl Acad. Sci. USA*, **111**, 4233–4238.
32. Perot, G., Soubeyran, I., Ribeiro, A., Bonhomme, B., Savagner, F., Boutet-Bouzamondo, N., Hostein, I., Bonichon, F., Godbert, Y. and Chibon, F. (2014) Identification of a recurrent STRN/ALK fusion in thyroid carcinomas. *PLoS One*, **9**, e87170.
33. Agrawal, N., Akbani, R., Aksoy, B.A., Ally, A., Arachchi, H., Asa, S.L., Auman, J.T., Balasundaram, M., Balu, S., Baylin, S.B. *et al.* (2014) Integrated genomic characterization of papillary thyroid carcinoma. *Cell*, **159**, 676–690.
34. Schwarz, J.M., Cooper, D.N., Schuelke, M. and Seelow, D. (2014) MutationTaster2: mutation prediction for the deep-sequencing age. *Nat. Methods*, **11**, 361–362.
35. Lee, J.J., Foukakis, T., Hashemi, J., Grimelius, L., Heldin, N.E., Wallin, G., Rudduck, C., Lui, W.O., Hoog, A. and Larsson, C. (2007) Molecular cytogenetic profiles of novel and established human anaplastic thyroid carcinoma models. *Thyroid*, **17**, 289–301.
36. Garcia-Rostan, G., Zhao, H., Camp, R.L., Pollan, M., Herrero, A., Pardo, J., Wu, R., Carcangiu, M.L., Costa, J. and Tallini, G. (2003) ras mutations are associated with aggressive tumor phenotypes and poor prognosis in thyroid cancer. *J. Clin. Oncol.*, **21**, 3226–3235.
37. Milosevic, Z., Pesic, M., Stankovic, T., Dinic, J., Milovanovic, Z., Stojsic, J., Dzodic, R., Tanic, N. and Bankovic, J. (2014) Targeting RAS-MAPK-ERK and PI3K-AKT-mTOR signal transduction pathways to chemosensitize anaplastic thyroid carcinoma. *Transl. Res.*, **164**, 411–423.
38. Ricarte-Filho, J.C., Ryder, M., Chitale, D.A., Rivera, M., Heguy, A., Ladanyi, M., Janakiraman, M., Solit, D., Knauf, J.A., Tuttle, R.M. *et al.* (2009) Mutational profile of advanced primary and metastatic radioactive iodine-refractory thyroid cancers reveals distinct pathogenetic roles for BRAF, PIK3CA, and AKT1. *Cancer Res.*, **69**, 4885–4893.
39. Xing, M. (2013) Molecular pathogenesis and mechanisms of thyroid cancer. *Nat. Rev. Cancer*, **13**, 184–199.
40. McFadden, D.G., Vernon, A., Santiago, P.M., Martinez-McFaline, R., Bhutkar, A., Crowley, D.M., McMahon, M., Sadow, P.M. and Jacks, T. (2014) p53 constrains progression to anaplastic thyroid carcinoma in a Braf-mutant mouse model of papillary thyroid cancer. *Proc. Natl Acad. Sci. USA*, **111**, E1600–E1609.
41. Charles, R.P., Silva, J., Iezza, G., Phillips, W.A. and McMahon, M. (2014) Activating BRAF and PIK3CA mutations cooperate to promote anaplastic thyroid carcinogenesis. *Mol. Cancer Res.*, **12**, 979–986.
42. Martin, M., Masshofer, L., Temming, P., Rahmann, S., Metz, C., Bornfeld, N., van de Nes, J., Klein-Hitpass, L., Hinnebusch, A.G., Horsthemke, B. *et al.* (2013) Exome sequencing identifies recurrent somatic mutations in EIF1AX and SF3B1 in uveal melanoma with disomy 3. *Nat. Genet.*, **45**, 933–936.
43. Ewens, K.G., Kanetsky, P.A., Richards-Yutz, J., Purrazzella, J., Shields, C.L., Ganguly, T. and Ganguly, A. (2014) Chromosome 3 status combined with BAP1 and EIF1AX mutation profiles are associated with metastasis in uveal melanoma. *Invest. Ophthalmol. Vis. Sci.*, **55**, 5160–5167.
44. Field, M.G. and Harbour, J.W. (2014) Recent developments in prognostic and predictive testing in uveal melanoma. *Curr. Opin. Ophthalmol.*, **25**, 234–239.
45. Yu, C., Luo, C., Qu, B., Khudhair, N., Gu, X., Zang, Y., Wang, C., Zhang, N., Li, Q. and Gao, X. (2014) Molecular network including eIF1AX, RPS7, and 14-3-3gamma regulates protein translation and cell proliferation in bovine mammary epithelial cells. *Arch. Biochem. Biophys.*, **564**, 142–155.
46. Hardt, M., Chantaravisoot, N. and Tamanoi, F. (2011) Activating mutations of TOR (target of rapamycin). *Genes Cells*, **16**, 141–151.
47. Roskoski, R. Jr. (2014) The ErbB/HER family of protein-tyrosine kinases and cancer. *Pharmacol. Res.*, **79**, 34–74.
48. Ross, J.S., Wang, K., Gay, L.M., Al-Rohil, R.N., Nazeer, T., Sheehan, C.E., Jennings, T.A., Otto, G.A., Donahue, A., He, J. *et al.* (2014) A high frequency of activating extracellular domain ERBB2 (HER2) mutation in micropapillary urothelial carcinoma. *Clin. Cancer Res.*, **20**, 68–75.
49. Kim, N., Hong, Y., Kwon, D. and Yoon, S. (2013) Somatic mutaome profile in human cancer tissues. *Genomics Inform.*, **11**, 239–244.
50. Eudy, J.D., Weston, M.D., Yao, S., Hoover, D.M., Rehm, H.L., Ma-Edmonds, M., Yan, D., Ahmad, I., Cheng, J.J., Ayuso, C. *et al.* (1998) Mutation of a gene encoding a protein with extracellular matrix motifs in Usher syndrome type IIa. *Science*, **280**, 1753–1757.
51. Yoshida, R., Miyashita, K., Inoue, M., Shimamoto, A., Yan, Z., Egashira, A., Oki, E., Kakeji, Y., Oda, S. and Maehara, Y. (2011) Concurrent genetic alterations in DNA polymerase proofreading and mismatch repair in human colorectal cancer. *Eur. J. Hum. Genet.*, **19**, 320–325.
52. Loeb, L.A. (2011) Human cancers express mutator phenotypes: origin, consequences and targeting. *Nat. Rev. Cancer*, **11**, 450–457.
53. Birkbak, N.J., Kochupurakkal, B., Izarzugaza, J.M., Eklund, A.C., Li, Y., Liu, J., Szallasi, Z., Matulonis, U.A., Richardson, A.L., Iglehart, J.D. *et al.* (2013) Tumor mutation burden forecasts outcome in ovarian cancer with BRCA1 or BRCA2 mutations. *PLoS One*, **8**, e80023.

54. Shcherbakova, P.V. and Kunkel, T.A. (1999) Mutator phenotypes conferred by MLH1 overexpression and by heterozygosity for mlh1 mutations. *Mol. Cell. Biol.*, **19**, 3177–3183.
55. Stulp, R.P., Herkert, J.C., Karrenbeld, A., Mol, B., Vos, Y.J. and Sijmons, R.H. (2008) Thyroid cancer in a patient with a germline MSH2 mutation. Case report and review of the Lynch syndrome expanding tumour spectrum. *Hered. Cancer Clin. Pract.*, **6**, 15–21.
56. Fagin, J.A., Matsuo, K., Karmakar, A., Chen, D.L., Tang, S.H. and Koeffler, H.P. (1993) High prevalence of mutations of the p53 gene in poorly differentiated human thyroid carcinomas. *J. Clin. Invest.*, **91**, 179–184.
57. Garcia-Rostan, G., Camp, R.L., Herrero, A., Carcangiu, M.L., Rimm, D.L. and Tallini, G. (2001) Beta-catenin dysregulation in thyroid neoplasms: down-regulation, aberrant nuclear expression, and CTNNB1 exon 3 mutations are markers for aggressive tumor phenotypes and poor prognosis. *Am. J. Pathol.*, **158**, 987–996.
58. Paes, J.E. and Ringel, M.D. (2008) Dysregulation of the phosphatidylinositol 3-kinase pathway in thyroid neoplasia. *Endocrinol. Metab. Clin. North Am.*, **37**, 375–387. viii–ix.
59. Cordenonsi, M., Montagner, M., Adorno, M., Zacchigna, L., Martello, G., Mamidi, A., Soligo, S., Dupont, S. and Piccolo, S. (2007) Integration of TGF-beta and Ras/MAPK signaling through p53 phosphorylation. *Science*, **315**, 840–843.
60. Guo, X. and Wang, X.F. (2009) Signaling cross-talk between TGF-beta/BMP and other pathways. *Cell Res.*, **19**, 71–88.
61. Holley, T., Lenkiewicz, E., Evers, L., Tembe, W., Ruiz, C., Gsponer, J.R., Rentsch, C.A., Bubendorf, L., Stapleton, M., Amorese, D. *et al.* (2012) Deep clonal profiling of formalin fixed paraffin embedded clinical samples. *PLoS One*, **7**, e50586.
62. Menon, R., Deng, M., Boehm, D., Braun, M., Fend, F., Boehm, D., Biskup, S. and Perner, S. (2012) Exome enrichment and SOLiD sequencing of formalin fixed paraffin embedded (FFPE) prostate cancer tissue. *Int. J. Mol. Sci.*, **13**, 8933–8942.
63. Schweppe, R.E., Klopper, J.P., Korch, C., Pugazhenthi, U., Benezra, M., Knauf, J.A., Fagin, J.A., Marlow, L.A., Copland, J.A., Smallridge, R.C. *et al.* (2008) Deoxyribonucleic acid profiling analysis of 40 human thyroid cancer cell lines reveals cross-contamination resulting in cell line redundancy and misidentification. *J. Clin. Endocrinol. Metab.*, **93**, 4331–4341.
64. Wennerberg, E., Pfefferle, A., Ekblad, L., Yoshimoto, Y., Kremer, V., Kaminskyy, V.O., Juhlin, C.C., Hoog, A., Bodin, I., Svjatoha, V. *et al.* (2014) Human anaplastic thyroid carcinoma cells are sensitive to NK cell-mediated lysis via ULBP2/5/6 and chemoattract NK cells. *Clin. Cancer Res.*, **20**, 5733–5744.